Classification of Glaucoma Image Using Supervised Classifiers and Segmentation of Blood Vessel

E. S. Vinothkumar[1], P. Hemavathy[2], Najeem Dheen Abdul Majeeth[3], V. Ramachandran[4],

P. Sundaravadivel[5*], R. Augustian Isaac[6]

Abstract: In this work, a variety of image processing approaches that are employed in the evaluation of the Cup to Disc ratio on the pre-processed retinal fundus pictures are discussed. The suggested method is divided into five main phases, including data collecting, picture pre-processing, segmentation of blood vessels, feature extraction, and classification for glaucoma detection by removing the blood vessel. First, the input photos are gathered from the DRIVE, HRF, DRIONS-DB, and STARE datasets, which stand for Structured Analysis of the Retina. The acquired retinal images are then cleaned up by median filtering and contrast limiting adaptive histogram equalisation techniques. Hybrid features are used to extract the feature values in order to improve classification performance. In the experimental phase, the proposed system improved the retinal blood vessel segmentation and classification up to 2% in comparison with other existing methods. All the experiments are evaluated through various performance indices like accuracy, sensitivity, specificity, precision, recall.

1. Introduction

For the diagnosis of disorders including glaucoma, diabetic retinopathy, macular degeneration, etc., blood vessel segmentation is used. Glaucoma is the condition that affects people the most frequently among these illnesses. IOP measurement, ONH, and retinal nerve fibre layer for the detection of visual field abnormalities are required for the diagnosis of glaucoma [1]. Medical diagnosis is accomplished through ophthalmic examinations. The fundus images only look at the areas of the image that are helpful for diagnosing the macula. By analysing the macula, age-related glaucoma is examined and detected

[1]Saveetha Engineering College, Thandalam, Chennai,
India, 602 105
Email: vinothkumar2k@gmail.com
ORCID: 0000-0001-5838-2898
[2]Saveetha Engineering College, Thandalam, Chennai,
India, 602 105.
Email: hemavathyp@saveetha.ac.in
ORCID: 0000-0002-5781-0616
[3]Saveetha Engineering College, Thandalam, Chennai,
India, 602 105.
Email: andheen@gmail.com
ORCID: 0000-0002-2314-5582
[4]Saveetha Engineering College, Thandalam, Chennai,
India, 602 105.
Email: ramachandranv@saveetha.ac.in
ORCID: 0009-0004-0294-2779
[5]Saveetha Engineering College, Thandalam, Chennai,
India, 602 105.
Email: sundar.me2009@gmail.com
ORCID: 0000-0003-1115-9490
*(Corresponding Author)
[6]Saveetha Engineering College, Thandalam, Chennai,
India, 602 105.
Email ID: sangam.naadu@gmail.com
ORCID: 0009-0004-6479-6885

[2]. Further explanations are provided regarding the causes of the disease and the requirement for blood vessel segmentation If not emptied, the aqueous humour in the eye's duct raises pressure inside the eye. IOP elevation sends signals to the brain that result in visual loss [3]. The screening uses distinguishing characteristics such blood vessels, the optic disc, the macula, etc. One of the causes of glaucoma, including blood vessel narrowing, occlusions, neovascularisation, etc., is changes in the anatomical structure of blood vessels. The eye's blood vessels reflect on evaluating the health of the body's organs. Along with segmenting blood vessels, screening procedures serve as the fundamental foundation model for the detection of retinal characteristics. Early detection of the glaucoma condition is necessary to stop visual loss as soon as feasible. Early detection of ocular problems will gradually reduce the risk of blindness. For the purpose of identifying glaucoma disease, the blood vessels in an eye's fundus picture are analysed and segmented [4]. The lesion appears bright and dark in the fundus picture, making it challenging to distinguish these areas. The macula, optic disc, optic cup, retina, and fovea are all parts of the eye's internal, opposite-facing surface. Patients with the condition typically have retinal blood vessels that are narrower than those of a healthy person [5]. Calculating the blood vessel area allows for the diagnosis of glaucoma; hence, any anatomical or structural alterations to the blood vessel serve as a sign of the condition. The automatic retinal vascular eye diagnosis is crucial in identifying systemic disorders. It is difficult to segment retinal blood vessels accurately and automatically [6]. A fundus image's

colour characteristics, diameter, and optic disc morphology are all examined during the segmentation of the blood vessels. The purpose of a mass eye exam is to diagnose and treat glaucoma early. Techniques for segmenting images were used to find lesions in the eyes that had been present for a few years, as well as retinal structures like the blood veins of the optic disc. The tissues in the retina are overlapped when retinal fundus images are acquired under various situations, which also affect the segmentation of the blood vessels and the optic disc, two important retinal tissues. On this result, K-means clustering is used to divide pixels into vessel and non-vessel clusters. Out of the two groups, the identified non-vessel group is subjected to an ensemble classification process using a root guided decision tree with bagging, however the vessel group is not processed because additional processing could lead to more vessels being incorrectly classified as non-vessels [7]. The outputs of the clustering and ensemble classification processes are combined to create the final segmented image. Using morphological approaches, the vessel segmentation output from the previous phase is post-processed.

2. Related Works

The majority of glaucoma detection systems in use today need on human involvement since examinations are often complex, time-consuming, and require qualified specialists [8]. Most of the time, manual examination of the retinal image results in incorrect diagnoses because of human error, which is typically brought on by visual tiredness [9-12]. Computer-aided design systems are created as a standard for screening and diagnosis in order to improve the diagnostic precision of screening retinal pictures [13]. Retinal image analysis is currently the subject of a large number of automated systems being developed for a variety of issues that are documented in the literature [14]. The majority of current IV techniques use computational algorithms, which heavily rely on computer use [15,16]. Increasing the segmentation and classification accuracy of glaucoma detection is the primary goal of this research [17]. In this study, supervised and unsupervised classifiers are used to segment and categorise the optic disc cup in order to detect glaucoma.

3. Proposed Method

The basic block diagram of the proposed Hybrid Intensity Features extraction methodology is shown in the Figure 1. The first step is the preprocessing that consists of contrast equalization and illumination correction. The input image is an RGB image utilizing only the green channel, as the blood vessels with retinal structures have high contrast. The pre-processed image uses the filtered image for segmentation of blood vessels.
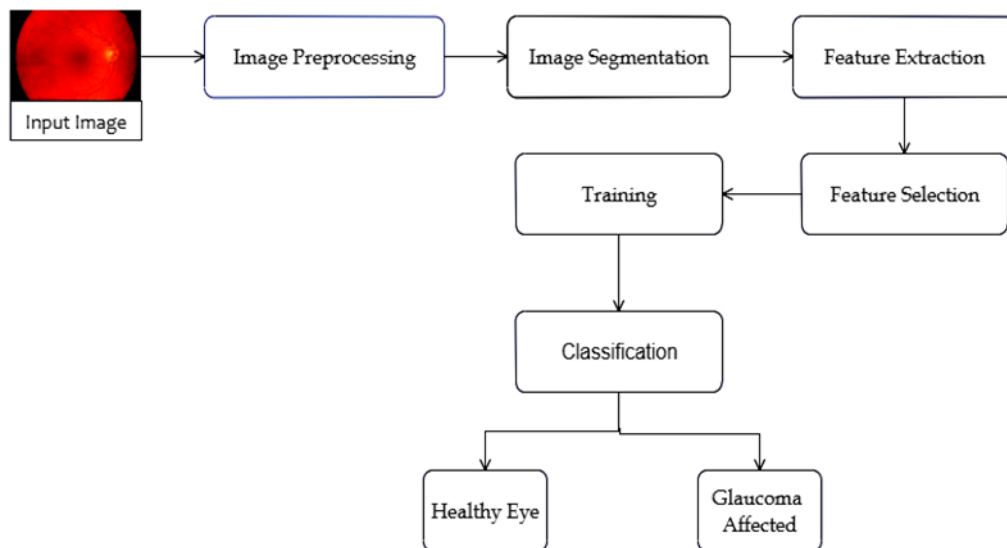

Fig. 1. Block diagram of the Proposed System

After segmentation, it is crucial to reduce resources in order to specify different traits. Desired image regions are isolated and features are found using the digitised image components. The classifier for the vessels categorises the picture that is subjected to filtering. Segmented vasculature is integrated with the subimages to represent the blood vessels. The pixels in the sub-image classify vessels later in the classification process to produce segmented vasculature.

3.1 Collection of Data

This section describes the dataset that was used to test the suggested method. Fundus photos from the standard dataset, which is publically accessible through programmes like STARE and DRIVE, are employed in the suggested

technique. The retinopathy photos from the screening programme were included in the DRIVE dataset [30]. A total of 400 diabetic individuals were photographed, ranging in age from 25 to 90. The 40 images that were chosen were all chosen at random[32]. 7 photos that showed the symptoms of mild diabetic retinopathy were randomly chosen. There were no symptoms of diabetic retinopathy in any of the 33 photos. The DRIVE dataset's retinal images are in the JPEG format. The STARE dataset consists of retina images are huge in number which are taken from Topcon TRV 50 fundus camera. The images are having resolution of 700 X 605 for 24-bit gray scale image. The STARE dataset includes a sizable number of retina images that were captured by a Topcon TRV 50 fundus camera. The photos are 24-bit grayscale photographs at a resolution of 700 x 605. The STARE

dataset included 20 each of a coloured retinal image and a ground-truth image. The retinal pictures displayed in Figure 2. (A-D) and STARE datasets are samples from the DRIVE and STARE datasets (E-H)[31].

Similar to this, 110 colour fundus images of the retina that were obtained for the High Resolution Fundus (HRF) database were chosen at random for the experiment.

Only a high quality scanner, like the HP-PhotoSmart-S20, was utilised because the photographs are in digital format. For the RGB format photos, a resolution of 600 x 400 was employed, along with 8 bits per pixel. Additionally, for healthy individuals, glaucoma patients, and each patient with diabetic retinopathy, 15 photos from the HRF public database are taken into account.
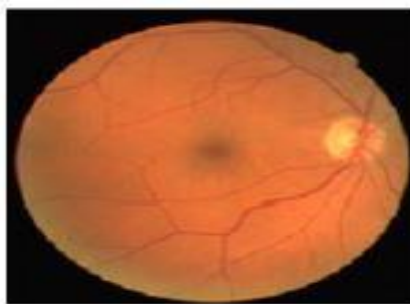
Sample Image for DRIVE Retinal Image
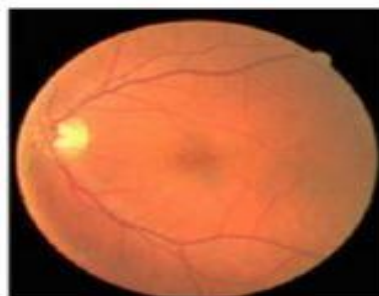
Sample Image for STARE Retinal Image

Sample Image for HAR Retinal Image

Fig. 2. Sample Images of the respective Database

3.2   Pre-Processing Techniques of Collected Image

The gathered data images are prepared for pre-processing, which removes artefacts that are undesirable for retinal fundus imaging. The pre-processing stage eliminates the noise that was gathered from the raw photos. The fundus camera is typically used to capture retinal pictures [29].

The retina has non-uniform background illumination; therefore, additional retinal images are taken of it. The intensity levels of the irregular background are different from those of the irregular background pixels. The grey level of the background pixel is typically non-uniform and higher than the pixel values of the vessels. During the pre-

processing stage, a powerful median filter is used to remove the backdrop that is not uniform.

3.3 Median Filtering

The median filter, a non-linear filter, will be used to offer smoothing classes while maintaining the edges. When the median filter, which contains the sharp details of the glaucoma image, is utilised, the smooth image is produced. The median value of all adjacent pixel values is used to get the pixel's middle value. Equation is used to compute the midpoint.

$$median[A(x) + B(x)] \neq median[A(x)] + median[B(x)] \tag{1}$$

Fundus pictures $A(x)$ and $B(x)$ are inputs in the equation above. The value of the median filter in the retinal image successfully gets rid of a number of unwanted sounds. The median filter is used by each pixel of the retinal image to represent its surroundings. The median filter modifies the neighbourhood pixel values for the mean and divides the pixel values by placing the neighbourhood pixels in numerical order. The entire pixel value has now taken the place of the middle pixel value. If there are an even number of pixels in the surrounding pixels, the two middle values of the pixel are used. Figure 3 shows the pre-processed image made from the retinal image.
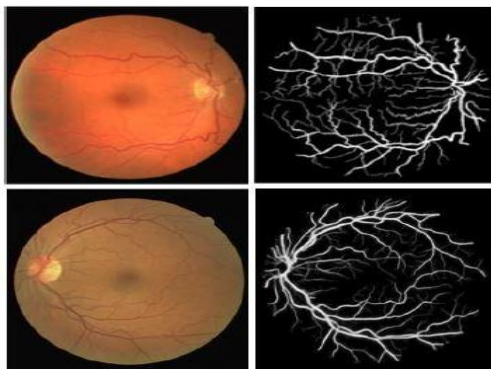
Fig. 3 (a). Input Retinal Image (b) Pre-processed Image using Median Filter

3.4 Segmentation Techniques

For segmentation, the blood vessels that make up the centre of the optic disc are dispersed around the retinal region. Given the interference between the optic disc and blood vessels, the segmentation of the blood vessels from the optic disc is crucial. Since the pixels were misdirected, the optic disc area misdetects blood vessels. The blood vessels are precisely segmented to be removed from the retinal image because they come from various parts of the optic disc. Different strategies are used to separate the photos based on their pixel content[19].

3.5 Techniques for Feature Extraction

The crucial features are those that turn data input into more informative qualities like colour, texture, shape, etc.

Glaucoma first manifests as changes in the optic disc and cup structures for a particular eye. Entropy, standard deviation, energy, and other parameters are extracted together with the picture and texture intensity. The classification of the image as healthy or abnormal is based on variations in the intensity and textural elements[20].
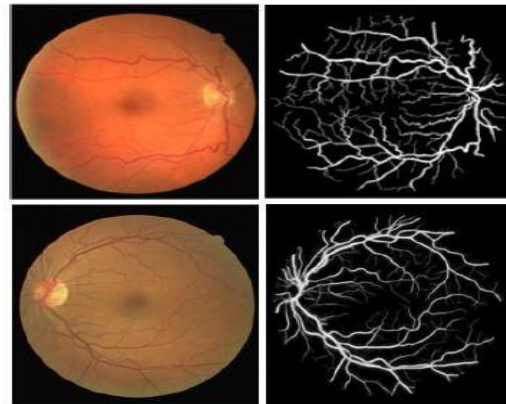
Fig. 4. Sample Segmented Retinal Blood Vessel Images

The classification process categorizes pixels into a digital image that distribute into data of classes. The data is used to classify as blood vessels or non-vessel glaucoma images are used to process classification for multispectral data. Indeed, the spectral pattern in the data is used for categorizing the numerical values. The techniques involved for the classification process is explained in the next sections.

3.6 Support Vector Machine

With the use of SVM, the retrieved features are now used to categorise the blood vessels as either normal or glaucoma blood vessels (Tuba, 2017). Because the classifier has discriminative properties in the hyper plane, it uses a supervised classification process. The input feature values produce the best model for creating training and testing samples of the features produced from the inputs. Applications that use dimensional data with a wide range include computer vision, image retrieval, medical image processing [18], signal processing, etc. The two-class restrictions are overcome by two-class problems like vapnikchervonenkis and the structural principles. The formula for the discriminant function is linear and reads as follows:. $x + a = 0$ these two optimal hyper-plane of two groups distinguishes samples free from the noise and mathematically expressed in

$$pi[W.x + a] - 1 \geq 0, i = 1,2,..D \tag{2}$$

3.7 Extreme Learning Machine Classifier

When compared to other back propagation networks, ELM is one of the Feed Forward Neural Networks that has hidden node layers of one or more[21]. The parameter is typically not used for tuning by the network nodes. According to research published in (Huang, 2012), SVM regression performs better than SVM. It enables the

selection of input weights at random, and computes outcomes analytically. Utilizing linearly the Single-Hidden Layer Feed Forward Neural network (SLFN). The weights are chosen at random using the output from the bias selection process. Analytically, the output matrices are used to determine the inverse operation[22].

$$f_L(x) = \sum_{i=1}^{L} \beta_i h_i(x) \qquad (3)$$

Where β_i is weight of the output of ith hidden node. Artificial neurons are used in the ELM's hidden layer to create fundamental functions and other training data. All non-constant bounded activation functions are implemented using ELM. With Back Propagation algorithms, the issue of irregular learning rate, over fitting, etc. is significantly less of a problem [23].

3.8 Random Forest

The key control element is considered for number of trees in the supervised classifier. The independent samples are the random vectors that are formed from arrangement of split trees in forest. The strength of trees and the correlation between them decide an error [24]. The trees are grown for each tree and the algorithms for classification are used and the Table 4.1 shows the parameter setting. The features generated are hybrid and are used for classification such as SVM, Random Forest, ELM with the parameters listed in the table 3.1. The abnormality is determined by finding the classifier accuracy [25].

Table 3.1. Classifier Parameter Setting

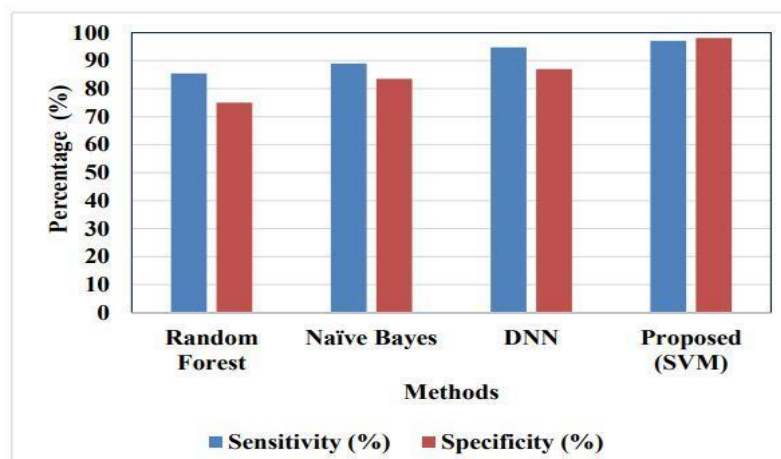| Classification Method	Setting The Parameters
SVM	Non-linear Kernel – REF with γ = 3
ELM	Hidden Layer = 1, with 250 training Cycles
Random Forest	Number of trees = 10

4. Results and Discussion

On the DRIVE, STARE, HRF, and DRIONS-DB datasets, the proposed segmentation method's effectiveness is assessed. Here, the proposed method's effectiveness is evaluated in terms of accuracy, kappa index sensitivity, and specificity.

4.1 Quantitative Analysis Performed For The Drive Dataset

The evaluation of the DRIVE dataset and comparison of performance evaluation with several classification approaches, such as DNN, Naive Bayes, and random forest, are covered in the current part. In the suggested methodology, the kappa index, accuracy, specificity[26], and sensitivity are examined. For training and testing purposes, the suggested model utilised 40% and 60% of retinal pictures, respectively. Results of the suggested classification methods are validated for that specific classifier. The suggested classifier CNN-SVM obtains 97.12% of sensitivity, and when compared to the current models, classifiers for DNN, Naive Bayes, and Random Forest achieved sensitivity of 94.76%, 89%, and 85.43%, respectively. Comparing the proposed classifier to the current models, CNN-SVM obtains 98.09% specificity, while DNN, Naive Bayes, and Random Forest only score 87%, 87%, and 75% specificity, respectively. Table 1.displays the tabulated data derived from experimentation, and Figure 3.displays a comparison graph of specificity and sensitivity.

Table 4.1. Performance comparison for Sensitivity and Specificity for DRIVE dataset

Methodologies	Random Forest	Naïve Bayes	DNN	Proposed SVM
Sensitivity (%)	85.43	89	94.76	97.12
Specificity (%)	75	83.5	87	98.09

Fig. 5. Comparison graph - Sensitivity V/S Specificity for DRIVE dataset

Additionally, compared to the previous models' classifiers, which achieved accuracy of 93.98% for DNN, 90.89% for Nave Bayes, and 91.22% for Random Forest, the proposed classifier CNN-SVM obtains 97.43% accuracy. The proposed classifier CNN-SVM achieves a Kappa index of 89.76%, and when compared to the current models, classifiers for DNN, Naive Bayes, and Random Forest achieved Kappa indices of 83.44%, 79.08%, and 79%, respectively. The experiment's tabulated values are displayed in Table 2, and Figure 4.displays a comparison graph of accuracy and kappa index.

Table 4.2. Performance Comparison for Accuracy and Kappa Index for DRIVE Dataset

Methodologies	Random Forest	Naïve Bayes	DNN	Proposed SVM
Accuracy (%)	72.03	87.33	92	96.89
Kappa Index (%)	86	79.55	85.45	88

Table 4.3. Performance Comparison of Specificity and Specificity for STARE dataset

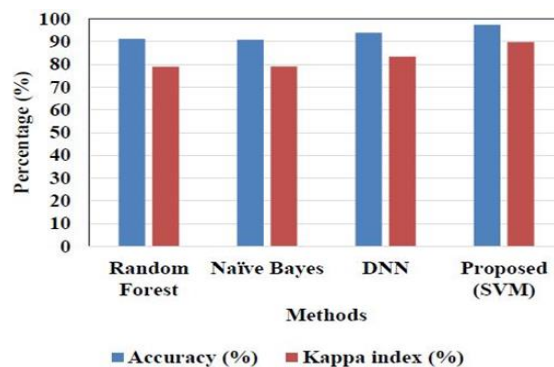| Methodologies	Random Forest	Naïve Bayes	DNN	Proposed SVM
Accuracy (%)	91.22	90.89	93.98	97.43
Kappa Index (%)	79	79.08	83.44	89.76

Fig. 6. Comparison graph - Accuracy and kappa index for DRIVE dataset

4.2 Quantitative Analysis Performed For Stare Dataset

The proposed method used the STARE database for the comparison of performance measures that are considered for classification. The results tabulated showed are validated and performed classification methodologies using various classifiers. The proposed classifier is CNN-SVM achieves 97.34% of sensitivity and compared with the existing models classifiers achieved sensitivity 91.77% for DNN, 86.95% for Naïve Bayes, and 72.33% for Random Forest. The proposed classifier is CNN-SVM achieves 97.49% of specificity and compared with the existing models classifiers achieved specificity 88.4% for DNN, 83% for Naïve Bayes, and 76.55 % for Random Forest. Table 4.3 shows the tabulated values obtained from experimentation and Figure 4.8 shows the specificity and sensitivity comparison graph[27].

In addition, the proposed classifier CNN-SVM achieves 96.89% of accuracy and compared with the existing models classifiers achieved 92% of accuracy for DNN, 87.33% for Naïve Bayes, and 72.03% for Random Forest. The proposed classifier CNN-SVM achieves Kappa index of 88% for the proposed method and compared with the existing models[28].

Table 4.4. Performance comparison for Accuracy and Kappa Index for STARE dataset

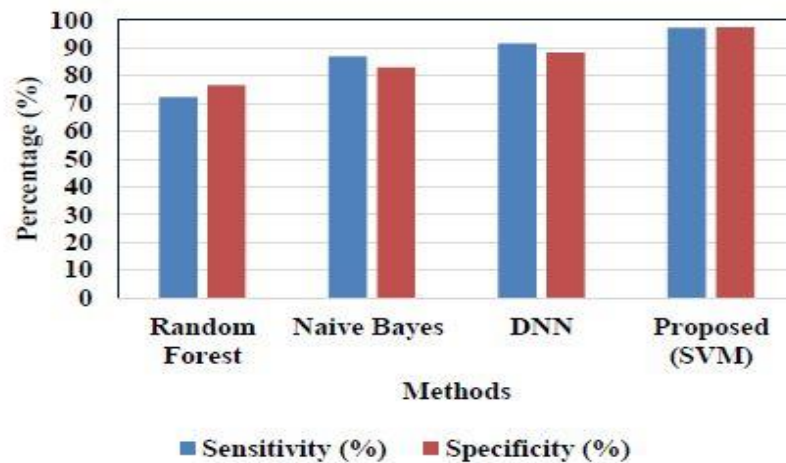| Methodologies	Random Forest	Naïve Bayes	DNN	Proposed SVM
Accuracy (%)	72.03	87.33	92	96.89
Kappa Index (%)	86	79.55	85.45	88

Fig. 7. Comparison graph- Specificity and Sensitivity for STARE dataset

The existing model classifiers achieved Kappa index 85.45% for DNN, 79.87% for Naïve Bayes, and 86% for Random Forest. Table 4.5 shows the tabulated values obtained from experimentation and Figure 8 shows the accuracy and Kappa index comparison graph.
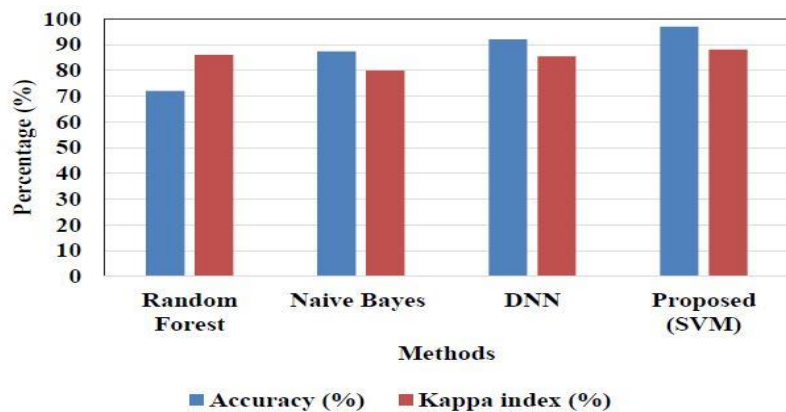

Fig. 8. Comparison graph Accuracy and kappa index for STARE Data Set

5. Conclusion

In essence, glaucoma is a group of diseases that permanently impair eyesight by destroying the optic nerve. This study offered a method for classifying retinal blood vessels by segmenting them. Data collection, picture pre-processing, segmentation, and feature extraction are all included in the proposed framework. The image is classified using the retrieved features, with each procedure having its own phase of execution. Performance of the suggested approach was assessed using openly accessible databases from DRIVE and STARE. When compared to conventional methods, the accuracy in blood vessel segmentation attained by the suggested method is higher. Using DRIVE Databases, the aberrant and normal image of glaucoma disease are classified using the appropriate segmentation and feature extraction approach. The unnecessary feature vectors were removed, and the remaining ones were divided into retinal blood vessels and non-vessels. The feature values were used to categorise aberrant and normal blood arteries using SVM, ELM, and Random Forest classifiers. The available strategy in glaucoma performs more effectively than the current approaches in terms of specificity, sensitivity, accuracy, and correlation coefficient.

References

[1] Acharya, UR, Dua, S, Du, X & Chua, CK. (2011), 'Automated diagnosis of glaucoma using texture and higher order spectra features', IEEE Transactions on information technology in biomedicine, vol. 15, no. 3, pp. 449-455.

[2] Acharya, UR, Ng, E, Eugene, LWJ, Noronha, KP, Min, LC, Nayak, KP &Bhandary, SV. (2015), 'Decision support system for the glaucoma using Gabor transformation', Biomedical Signal Processing and Control, vol. 15, pp. 18-26.

[3] Akram, MU & Khan, SA. (2013), 'Multilayeredthresholding-based blood vessel segmentation for screening of diabetic retinopathy', Engineering with computers, vol. 29, no. 2, pp. 165-173.

[4] Akram, MU, Tariq, A, Khalid, S, Javed, MY, Abbas, S &Yasin, UU. (2015), 'Glaucoma detection using novel optic disc localization, hybrid feature set and classification techniques', Australasian physical & engineering sciences in medicine, vol. 38, no. 4, pp. 643-655.

[5] Al-Bander, B, Al-Nuaimy, W, Al-Taee, MA &Zheng, Y. (2017), 'Automated glaucoma diagnosis using deep learning approach', in 2017 14th International Multi-Conference on Systems, Signals & Devices (SSD), pp. 207-210.

[6] Balasubramanian, T, Krishnan, S, Mohanakrishnan, M, Rao, KR, Kumar, CV &Nirmala, K. (2016), 'HOG feature based SVM classification of glaucomatous fundus image with extraction of blood vessels', in 2016 IEEE Annual India Conference (INDICON), pp. 1-4.

[7] Banister, K, Boachie, C, Bourne, R, Cook, J, Burr, JM, Ramsay, C, Garway-Heath, D, Gray, J, McMeekin, P & Hernández, R. (2016), 'Can automated imaging for optic disc and retinal nerve fiber layer analysis aid glaucoma detection?', Ophthalmology, vol. 123, no. 5, pp. 930-938.

[8] Benzebouchi, N, Azizi, N &Bouziane, S. (2018), 'Glaucoma diagnosis using cooperative convolutional neural networks', International Journal of Advances in Electronics and Computer Science, vol. 5, no. 1, pp. 31-36.

[9] Bhartiya, S, Ichhpujani, P & Gandhi, M. (2019), 'The Glaucoma Treatment Paradigm: An Overview', in Glaucoma Drainage Devices, Springer, pp. 1-6.

[10] Bhowmik, D, Kumar, KS, Deb, L, Paswan, S &Dutta, A. (2012), 'Glaucoma-A Eye Disorder Its Causes, Risk Factor, Prevention and Medication', The Pharma Innovation, vol. 1, no. 1, Part A, p. 66.

[11] Bock, R, Meier, J, Nyúl, LG, Hornegger, J & Michelson, G. (2010), 'Glaucoma risk index: automated glaucoma detection from color fundus images', Medical image analysis, vol. 14, no. 3, pp. 471-481.

[12] Carrillo, J, Bautista, L, Villamizar, J, Rueda, J & Sanchez, M. (2019), 'Glaucoma detection using fundus images of the eye', in 2019 XXII Symposium on Image, Signal Processing and Artificial Vision (STSIVA), pp. 1-4.

[13] Chai, Y, Liu, H &Xu, J. (2018)., 'Glaucoma diagnosis based on both hidden features and domain knowledge through deep learning models', Knowledge-Based Systems, vol. 161, pp. 147-156.

[14] Chaikitmongkol, V, Khunsongkiet, P, Patikulsila, D, Ratanasukon, M, Watanachai, N, Jumroendararasame, C, Mayerle, CB, Han, IC, Chen, CJ &Winaikosol, P. (2018), 'Color fundus photography, optical coherence tomography, and fluorescein angiography in diagnosing Polypoidal Choroidalvasculopathy', American Journal of Ophthalmology, vol. 192, pp. 77-83.

[15] Chang, DS, Arora, KS, Boland, MV, Supakontanasan, W & Friedman, DS. (2013), 'Development and validation of an associative model for the detection of glaucoma using pupillography', American journal of ophthalmology, vol. 156, no. 6, pp. 1285-1296. e1282.

[16] Chaudhuri, S, Chatterjee, S, Katz, N, Nelson, M &Goldbaum, M. (1989), 'Detection of blood vessels in retinal images using two-dimensional matched filters', IEEE Transactions on medical imaging, vol. 8, no. 3, pp. 263-269.

[17] Chen, X, Xu, Y, Wong, DWK, Wong, TY & Liu, J. (2015), 'Glaucoma detection based on deep convolutional neural network', in 2015 37th annual international conference of the IEEE engineering in medicine and biology society (EMBC), pp. 715-718.

[18] Rajasekaran, A. S., Yuvaraj, D., & Maria, A. (2022, March). Secure Authentication Scheme for Medical care applications based on IoT. In 2022 International Conference on Emerging Smart Computing and Informatics (ESCI) (pp. 1-5). IEEE.

[19] Santhi, R., & Yuvaraj, D. (2017). Content-Based Image Retrieval in Cloud Using Watermark Protocol and Searchable Encryption.

[20] Yuvaraj, D. ., Alnuaimi, S. S. ., Rasheed, B. H. ., Sivaram, M. ., & Porkodi, V. . (2024). Ontology Based Semantic Enrichment for Improved Information Retrieval model. International Journal of Intelligent Systems and Applications in Engineering, 12(15s), 70–77.

[21] Krishnan, S. N., Yuvaraj, D., & Mathusudhanan, S. M. S. (2019). Novel Feature Extraction Methods for Effective Texture Image And Data Classifications. Journal of Electrical Engineering, 19(2), 10-10.

[22] D.Yuvaraj, and S. Hariharan, "Content-based image retrieval based on integrating region segmentation and colour histogram", The International Arab Journal of Information Technology, 2(11), 12, 2016.

[23] Ahamed, B. B., Yuvaraj, D., & Priya, S. S. (2019). Image Denoising With Linear and Non-linear Filters. In 2019 International Conference on Computational Intelligence and Knowledge Economy (ICCIKE) (pp. 806-810). IEEE.

[24] Geetha, K., Yuvaraj, D.,(2018).A Novel Shape Feature Extraction Technique for Content-Based Image Retrieval (CBIR) Systems, International Journal of advance Science and Technology,28(2),158-169.

[25] Yuvaraj, D., Sivaram, M., Karthikeyan, B., & Abdulazeez, J. (2019). Shape, colour and texture-based CBIR system using the fuzzy logic

classifier. CMC-Computers Materials & Continua, 59(3), 729-739.

[26] Sundara Vadivel, P., Yuvaraj, D., Navaneetha Krishnan, S., & Mathusudhanan, S. R. (2019). An efficient CBIR system based on colour histogram, edge, and texture features. Concurrency and Computation: Practice and Experience, 31(12), e4994.

[27] RajeshKumar, N., Yuvaraj, D., Manikandan, G., BalaKrishnan, R., Karthikeyan, B., Narasimhan, D., & Raajan, N. R. (2020). Secret Image Communication Scheme Based on Visual Cryptography and Tetrolet Tiling Patterns. CMC-Computers Materials & Continua, 65(2), 1283-1301.

[28] D.Yuvaraj, Salar Faisal Noori, Subbiah Swaminathan, (2021) Multi-perspective scaling convolutional neural networks for high-resolution MRI brain image segmentation, Materials Today: Proceedings

[29] Krishnan, R. B., Yuvaraj, D., Devi, P. S., Chooralil, V. S., Kumar, N. R., Karthikeyan, B., & Manikandan, G. (2023). An Improved Steganographic Scheme Using the Contour Principle to Ensure the Privacy of Medical Data on Digital Images. Computer Systems Science & Engineering, 46(2).

[30] Sambandam, P., Yuvaraj, D., Padmakumari, P., & Swaminathan, S. (2023). Deep attention based optimized Bi-LSTM for improving geospatial data ontology. Data & Knowledge Engineering, 144, 102123.

[31] Yuvaraj, D., Sampath, A. K., Shanmugapriya, N., Samatha, B., Arun, S., & Thiyagarajan, R. (2022, October). Medical Image Segmentation of Bio-medical Images with Deep Convolution Neural Networks using Ensemble Approach. In 2022 3rd International Conference on Smart Electronics and Communication (ICOSEC) (pp. 1041-1049). IEEE.

[32] Yuvaraj, D., Dinesh, M., Sivaram, M., & Nageswari, S. (2022). An efficient data mining process on temporal data using relevance feedback method. World Review of Science, Technology and Sustainable Development, 18(1), 20-30